Cartesian coordinates scaffold stable spatial perception over time

Minghao Luo
School of Psychological and Cognitive Sciences, Peking University, Beijing, China
PKU-IDG/McGovern Institute for Brain Research, Peking University, Beijing, China
Beijing Key Laboratory of Behavior and Mental Health, Peking University, Beijing, China

Huihui Zhang
School of Psychological and Cognitive Sciences, Peking University, Beijing, China
PKU-IDG/McGovern Institute for Brain Research, Peking University, Beijing, China
Beijing Key Laboratory of Behavior and Mental Health, Peking University, Beijing, China

Huan Luo
School of Psychological and Cognitive Sciences, Peking University, Beijing, China
PKU-IDG/McGovern Institute for Brain Research, Peking University, Beijing, China
Beijing Key Laboratory of Behavior and Mental Health, Peking University, Beijing, China

Visual systems exploit temporal continuity principles to achieve stable spatial perception, manifested as the serial dependence and central tendency effects. These effects are posited to reflect a smoothing process whereby past and present information integrates over time to decrease noise and stabilize perception. Meanwhile, the basic spatial coordinate—Cartesian versus polar—that scaffolds the integration process in two-dimensional continuous space remains unknown. The spatial coordinates are largely related to the allocentric and egocentric reference frames and presumably correspond with early and late processing stages in spatial perception. Here, four experiments consistently demonstrate that Cartesian outperforms polar coordinates in characterizing the serial bias—serial dependence and central tendency effect—in two-dimensional continuous spatial perception. The superiority of Cartesian coordinates is robust, independent of task environment (online and offline task), experimental length (short and long blocks), spatial context (shape of visual mask), and response modality (keyboard and mouse). Taken together, the visual system relies on the Cartesian coordinates for spatiotemporal integration to facilitate stable representation of external information, supporting the involvement of allocentric reference frame and top-down modulation in spatial perception over long time intervals.

Introduction

Localizing objects in space, as one of the fundamental purposes of vision, is challenging because visual inputs to the retina are constantly varied either by self-motion, such as eye movements and head motion, or by changes in the outside world (Whitney, 2002). Meanwhile, our spatial perception effortlessly undergoes continuous and stable spatiotemporal experiences instead of a series of frozen temporal moments. A key strategy our visual perception employs is the so-called temporal continuity principle, which assumes that the environment would be similar to the one moments ago without abrupt changes in between (Fischer & Whitney, 2014; Rucci, Ahissar, & Burr, 2018). According to this principle, our brain integrates spatial information over time to stabilize spatial perception, and an intriguing relevant phenomenon is the "serial dependence" effect, that is, the perceived spatial location of a target in the current trial would be attracted to that in previous trials

Citation: Luo, M., Zhang, H., & Luo, H. (2022). Cartesian coordinates scaffold stable spatial perception over time. *Journal of Vision*, *22*(8):13, 1–13, https://doi.org/10.1167/jov.22.8.13.

https://doi.org/10.1167/jov.22.8.13 Received February 14, 2022; published July 20, 2022 ISSN 1534-7362 Copyright 2022 The Authors

This work is licensed under a Creative Commons Attribution-NonCommercial-NoDerivatives 4.0 International License.

(Bliss, Sun & D'Esposito, 2017; Burr & Cicchini, 2014; Fischer & Whitney, 2014; Manassi et al., 2018; Manassi & Whitney, 2022). In addition to being influenced by recent trials, our spatial perception also tends to be driven to the averaged location across a much longer temporal span, namely, the "central tendency" effect (Allred et al., 2016; Petzschner, Glasauer & Stephan, 2015; Sheth & Shimojo, 2001; Sciutti et al., 2012).

The serial dependence effect has been viewed as an adaptive smoothing process by forming a continuity field over space and time (Fischer & Whitney, 2014; Liberman et al., 2014), yet the basic spatial coordinates (Cartesian vs. polar) underlying this spatiotemporal continuity kernel remains obscure. The answer is closely related to reference frames exploited in spatial perception (Collins, 2019; Drissi-Daoudi et al., 2020; Fischer & Whitney, 2014; Klatzky, 1998; Mikellidou, Cicchini, & Burr, 2021). Specifically, in an allocentric reference frame, spatial perception would entail Cartesian coordinates to form optimal global representations and stabilize visual experiences (Gallistel, 1990; Yang, 2018), whereas an egocentric perspective would be more retinotopic and eye centered to maximize discrimination of visual features over time, thus favoring the polar coordinates (Zetzsche, Krieger, & Wegmann, 1999). The Cartesian versus polar coordinates, given their respective associations with late and early visual processing, might also correspond with the attractive and repulsive serial dependence, respectively (Fritsche, Mostert, & de Lange, 2017; Fritsche, Spaak, & De Lange, 2020; Pascucci et al., 2019).

The present study aims to examine the human stable spatial perception from two new perspectives: continuous two-dimensional (2D) space and the underlying spatial coordinates. By using a spatial location reproduction task within a 2D continuous space and measuring the serial dependence and central tendency, we demonstrate, in four experiments, that the Cartesian coordinates better characterize the spatial bias effect, compared with the polar coordinates. The role of Cartesian coordinates is robust and consistent, independent of task environment (online and offline tasks), experimental length (short and long blocks), spatial context (shape of the visual mask), and response modality (keyboard and mouse). Taken together, in a 2D continuous space, the visual system tends to rely on the Cartesian coordinates to stabilize and update spatial perception over time.

Methods

We conducted four experiments to systematically investigate the way of 2D spatial representation (Cartesian or polar coordinates) across time by examining location serial dependence and central tendency effects. In experiment 1, subjects were instructed to report both spatial location and orientation of a Gabor patch in each trial. Accordingly, we examined the serial dependence effect for both spatial location and orientation. The purpose of the orientation task was to validate the data quality and analysis, because the orientation serial dependence effect has been widely shown in previous studies. In experiments 2, 3, and 4, we only examined the location serial dependence effect. Experiments 1 and 4 were conducted in the laboratory. Because of the coronavirus disease 2019, experiments 2 and 3 were conducted online, and we used PsychoPy3 (Peirce et al., 2019) to build the experiments and ran them on the online platform pavlovia.org. Participants completed the experiment in a web browser on their PC, participating via mobile phone or tablet was not permitted.

Participants

The sample size was determined based on previous serial dependence in orientation reproduction studies (Fritsche et al., 2017). Twenty-three volunteers (six males), aged from 19 to 25 years, participated in experiment 1. For experiment 4, we recruited 27 participants (11 males, aged 18–24 years). They all have normal or corrected-to-normal visions. For experiments 2 and 3, we respectively recruited 398 and 409 participants online through prolific.co. All participants in the four experiments were naive to the purpose of the experiment, and they received compensation for participation. The study was approved by the Departmental Ethics Committee of Peking University, and it was conducted in accordance with the Declaration of Helsinki. Participants gave informed consent before the experiments.

Apparatus and materials

The Gabor patch had a spatial frequency of two cycles per degree, with a peak contrast of 25% Michelson and a 0.4° standard deviation Gaussian contrast envelope. The square noise patch was 15° in diameter and consisted of white noise smoothed with a 0.91° standard deviation Gaussian kernel. The response bar was white, 0.2° in width, and windowed in the same 0.4° standard deviation Gaussian contrast envelope. The round fixation dot was 0.2° in diameter and was always presented at the center of the screen. All materials were presented on a gray background (RGB: 127, 127, 127). The experiment was conducted on a 27-in LCD monitor with a refresh rate of 60 Hz. A chinrest was used to keep participants' viewing distance at 57 cm. All the experimental programs were

developed with MATLAB (MathWorks, Natick, MA) and Psychophysics Toolbox (Brainard, 1997; Pelli, 1997).

Design and procedure

Experiment 1

In experiment 1, participants needed to reproduce both the orientation and location of the Gabor patch presented at the beginning of each trial. After being informed of the task, participants did 10 practice trials that were the same as the formal trial. In the following formal experiment, each participant did 1,000 trials separated into 20 blocks. They took a break between blocks.

The Gabor patch was presented within a circular area that was centered at the fixation dot and was 15° in diameter. In each trial, the location of the Gabor patch was sampled randomly from the uniform distribution within the round area, and its orientation was sampled randomly from the uniform distribution between 0° and 180°. The location and orientation of the response bars were also randomly sampled in the same way, independent of those of the Gabor patches.

As shown in Figure 1A, participants viewed a Gabor patch for 500 ms while maintaining the fixation at the central white dot. A mask was next presented for 1,000 ms, followed by the response bar. Participants used keys 'w' (up), 's' (down), 'a' (left), and 'd' (right) to adjust the location of the response bar, and used keys '←' and '→' to rotate the bar to reproduce the orientation of the Gabor patch. Once the adjustment was done, participants pressed the space key to finish the current trial. The order of the location and the orientation adjustments were not a requirement.

Experiments 2 and 3

Experiments 2 and 3 were conducted online, and participants only performed the spatial location reproduction task. Each participant finished 50 trials, which took about 7 minutes, to ensure the appropriate experimental length for online experiments. Moreover, the small number of trials also helps us to examine whether the results rely on extensive learning or could occur automatically.

One potential problem of the online experiment was that the viewing distance and the monitor parameters varied among participants. To this end, we customized the stimulus size in pixels to keep their size equal in visual angle. Viewing distances and screen sizes were estimated by a virtual chinrest (Li et al., 2020) that consisted of two tasks. The first task was the card matching task, during which participants placed a credit card or a card of equal size on the screen and adjusted the image size on the screen to match the real-world card. The card size in pixel was denoted by parameter $\boldsymbol{a}$. The second task was the blind spot task, in which participants fixed their eyesight on a black square while a red dot was moving from the center to left. They were asked to press keys as soon as they could not see the dot (at the blind spot). The length that the dot traveled through in pixel was denoted by parameter $\boldsymbol{s}$. Because the blind spot position is constant among people ($\boldsymbol{\theta}$, about 13.5°), we could calculate the viewing distance, by:

$$Viewing\ distance\ (mm) = \frac{Card\ size\ (mm)\ \times s}{\tan\theta \times a}$$

For a stimulus with δ (visual degree) in size, its size in pixel was:

$$Size\ \ (pixel) = \frac{\tan\delta \times a \times Viewing\ distance\ \ (mm)}{Card\ size\ \ (mm)}$$

Screen parameters and viewing distances were measured first, followed by instructions and six practice trials with feedback. After practice, participants performed 50 formal trials.

Experiment 2 aimed to examine if the preference for Cartesian coordinates could be formed within a short time (only 50 trials per participant). Experiment 2 used the same task procedure as that in experiment 1, except that the target stimulus was a red dot of 0.4° in diameter instead of Gabor patches (Figure 2A left).

Experiment 3 examined if the preference for Cartesian coordinates arises from the shape of the mask. Instead of a square mask used in experiments 1 and 2, we truncated the square mask into a round mask that was 15° in diameter. The other stimuli and procedures remained the same as those in experiment 2.

Experiment 4

In previous experiments, the keyboard responses might implicitly create a Cartesian coordinate. For instance, the trajectories of key response 'w,' 's,' 'a,' and 'd' were in a quadrangular grid-like form. Experiment 4 aimed to examine if the preference for Cartesian coordinates arises from the keyboard response modality. To this end, we replaced the keyboard response with a mouse response, which was free in trajectory and did not have a bias to either of the two coordinates. At the response stage, a mouse cursor appeared at a random position, after which participants clicked a position to reproduce the location, and the red dot was then displayed. The response location could be revised by a new click, and when the adjustment was done, participants pressed the 'space' key to end the current trial. Other stimuli and procedures in

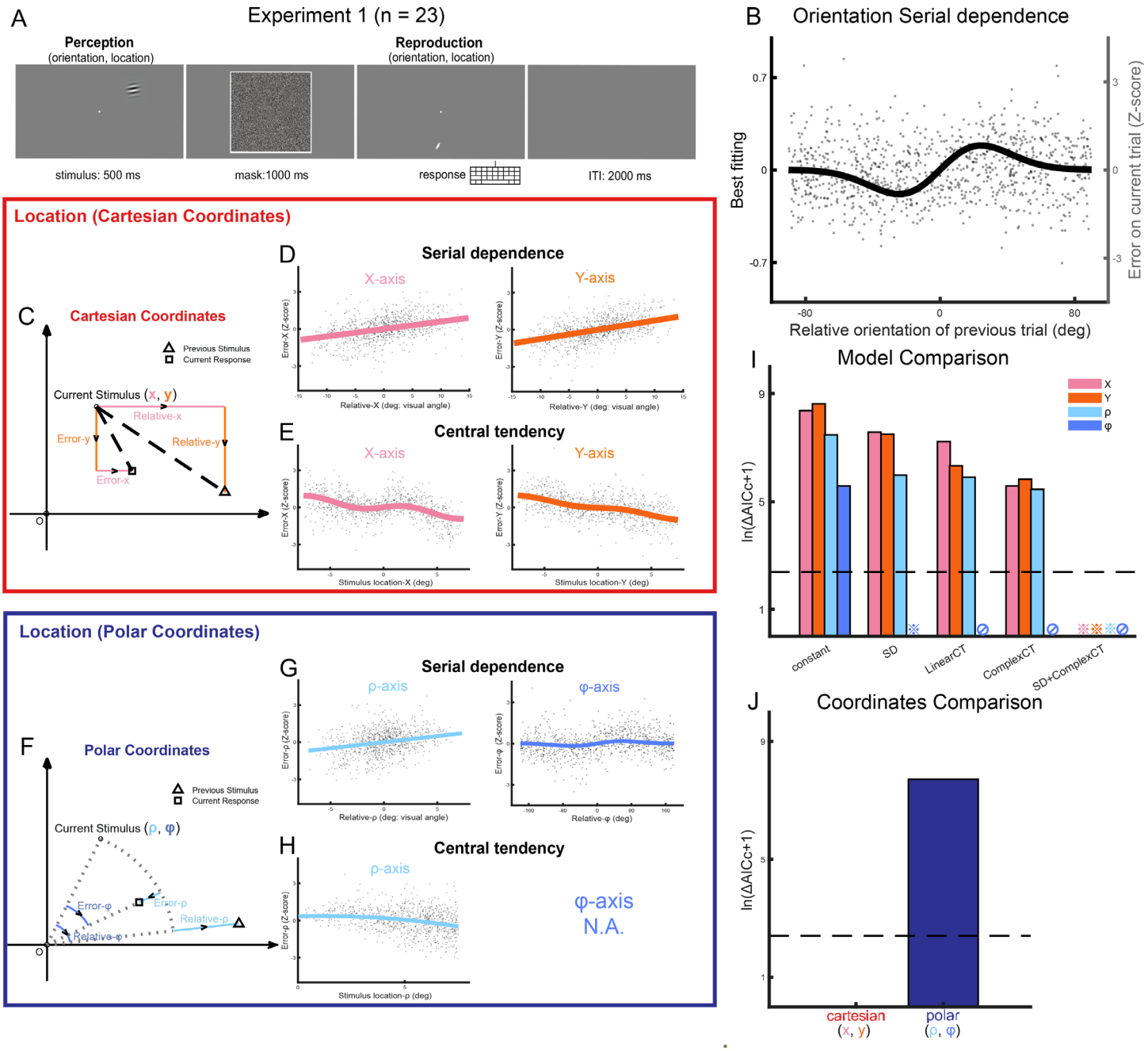

Figure 1. Experiment 1 paradigm, quantifying spatial bias by Cartesian and Polar coordinates, and model comparisons. (A) Participants performed a location and orientation reproduction dual-task on a Gabor stimulus occurring at a random location in a 2D continuous space, followed by a square mask. During the reproduction stage, subjects adjusted the position and the orientation of a white bar using keyboards to match the location and orientation of the Gabor stimulus during the perception stage. (B) Pooled results across subjects ($N = 23$) for orientation serial dependence. The *x* axis represents the difference between the current Gabor orientation and that in the preceding trial. The *y* axis represents the difference between the reported orientation and the true orientation in the current trial. The black curve denotes the fitted DoG curve across subjects. The gray points denote all the trials from one representative subject. (C–E) Serial dependence and central tendency effect on spatial perception in Cartesian coordinates. (C) Illustration of quantifying spatial bias at *x* and *y* axis. (D) Pooled serial dependence effect across subjects on spatial location at the *x* axis (left) and the *y* axis (right). The straight lines denote the best fitting linear trend. The gray dots represent all the trials from one representative subject in (B). (E) The same as (D), but for central tendency effect. (F–H) Serial dependence and central tendency effect on spatial perception in Polar coordinates. (F) Illustration of quantifying spatial bias at the ρ axis and the φ axis. (G–H) The same as (DE) but in the polar coordinates. Note that φ is not applicable to quantify central tendency effect. (I) Model comparison (Constant, SD, linear CT, complex CT, SD + complex CT) for four parameters (Cartesian coordinates: *x* and *y*; polar coordinates: ρ and φ). ※, best

→

←
model with the lowest AICc; ⊘, nonapplicable. The ΔAICc is calculated by subtracting the lowest AICc. Dashed line denotes threshold (log-transition of ΔAICc = 10) (J) Model comparison between Cartesian and polar coordinates. The dashed line denotes threshold (log-transition of ΔAICc = 10).

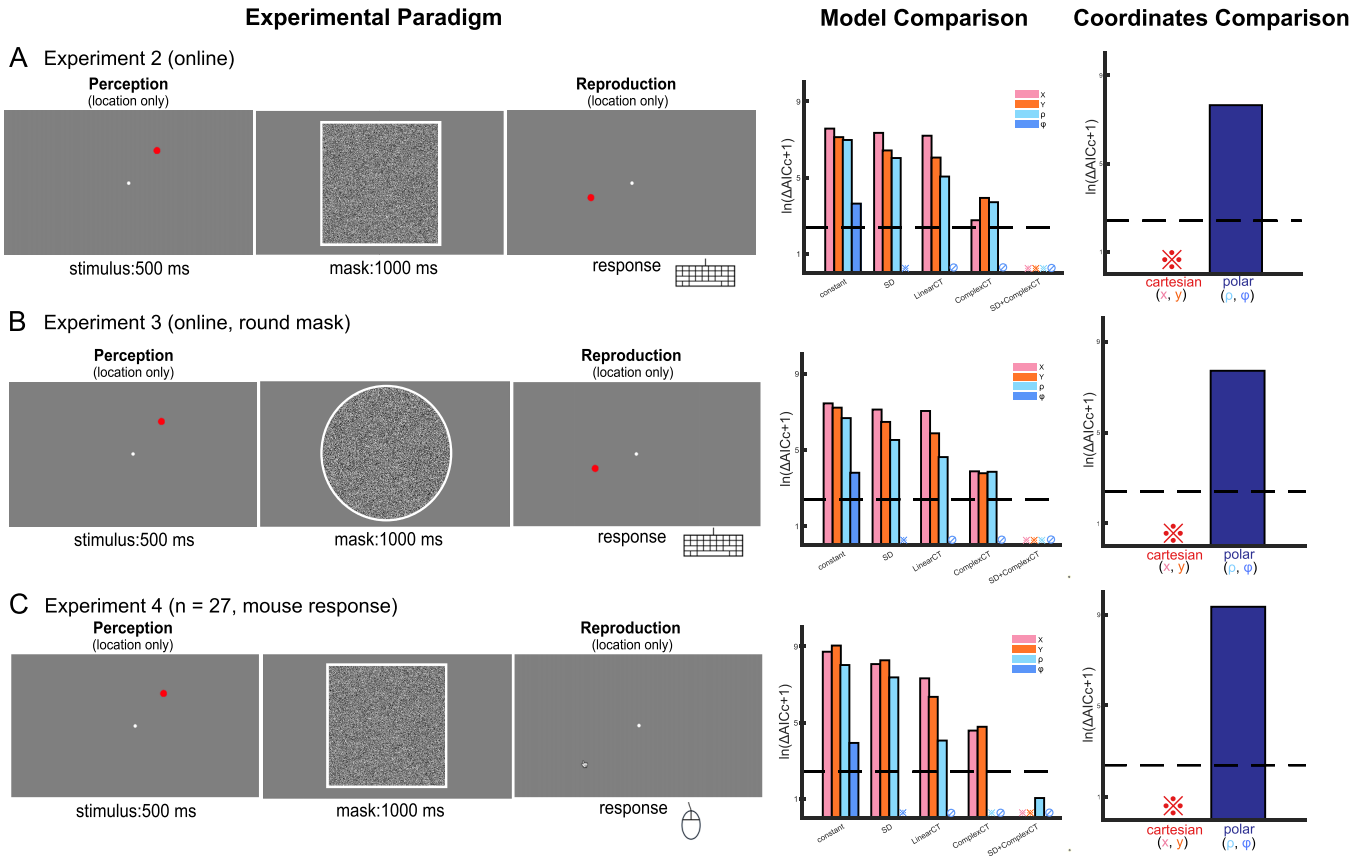

Figure 2. Robust function of Cartesian coordinates in serial bias in 2D continuous spatial perception (experiments 2–4) (A) Experiment 2 (online experiment, short block, keyboard response). (Left) Participants maintained their fixation on the central point and were presented with a red dot at random locations in a 2D continuous space, followed by a square mask. During the reproduction stage, subjects adjusted the position of the red dot with keyboards to match the red dot position during the perception stage. (Middle and right) model comparison results for experiment 2, with the same setting as Figure 1IJ. (B) Experiment 3 (online experiment, short block, keyboard response). Left: Subjects performed the same task as experiment 2 but with a round-shape mask. (Middle and right) Model comparison results for experiment 3, with the same setting as Figure 1IJ. (C) Experiment 4 (offline experiment, long blocks, mouse response). (Left) Subjects performed the same task as experiment 2, but by using a mouse. (Middle and right) Model comparison results for experiment 4, with the same setting as Figure 1IJ.

experiment 4 remained the same as in experiment 2. Each participant performed 1,000 trials divided into 20 blocks.

Data analysis

All data were analyzed using custom MATLAB (MathWorks) codes and additional functions from the Statistics and Machine Learning Toolbox, Optimization Toolbox, and Parallel Computing Toolbox. We analyzed how the past influences the current visual perception. For serial dependence effect, we limited "previous influence" to the 1-back trial to maximize its effect (Fischer & Whitney, 2014) in all four experiments. Because the serial dependence effect existed in consecutive trials (1-back), the first trial of each block was excluded, and the remaining 980 trials were thus obtained per participant in experiments 1 and 4, and 49 trials were obtained in experiments 2 and 3.

For the central tendency effect, we calculated its effect for all noncircular variables in all experiments.

Serial dependence in orientation perception

We calculated the response error in orientation (**error-ori**, responded orientation minus stimulus orientation) and relative orientation of previous trial (**relative-ori**, stimulus orientation in previous trial minus stimulus orientation in current trial). To quantify the serial dependence effect, we used the well-established Gaussian derivative (DoG) function (e.g., see Fischer & Whitney, 2014) to fit the data, given by:

$$y = awce^{-(wx)^2} + b \quad (1)$$

Here, x is **relative-ori**, y is **error-ori**, a is the amplitude of the curve peak, w scales the curve width, c is the constant $\sqrt{2}/e^{-0.5}$ scaling the curve to make a parameter equal to the peak amplitude, and b describes the vertical shifts along the y axis. We combined all participants' data into aggregated data for model fitting. Note that we normalized response error (**error-ori**) within participants to reduce variability among participants, and thus the dependent variable would be the z-score of **error-ori**.

Serial dependence in location perception

The 2D space can be described using two different coordinate systems, Cartesian or polar. Cartesian coordinates consist of x and y axes, with each location being represented by a pair of numerical coordinates. Polar coordinates consist of ρ (**distance**) and φ (**angle**) axes, characterizing a location by its distance from a reference point and the angle from a reference direction. The former is a grid-like coordinate system and the latter is a radial-like one. Notably, the two coordinate systems share the same original point, that is, the center of the screen.

The response error in location was defined as the vector from the stimulus location to the responded location (error-loc). The relative location of previous trial was defined as the vector from the current stimulus location to the previous stimulus location (relative-loc). We then projected them onto two axes. For Cartesian coordinates, we obtained the projection of error-loc on the x axis, **error-x,** and projection of error-loc on the y axis, **error-y**, respectively. The projection of the relative-loc onto the x and y axes resulted in **relative-x** and **relative-y** (Figure 1C). For polar coordinates, the projections onto the ρ axis were **error-ρ** and **relative-φ**, and the projections onto the φ axis were **error-ρ** and **relative-φ** (Figure 1F).

The variables on the x, y, and ρ axes are in noncircular forms, and the variable on the φ axis is circular ranging from –180° to 180°. These two kinds of variables exhibit different relationships between "**relative**" and "**error**." For the circular variable on the φ axis, it is in DoG form (Manassi et al., 2018); the circular variable for orientation in previous studies (Fischer & Whitney, 2014). For the noncircular variables on the x, y, and ρ axes, the relationships are in a linear form as an approximation of the DoG function whereby independent variables are restricted to a range of small values, corresponding with the limited space (e.g., Motala, Zhang, & Alais, 2020).

We fitted the relationship between "**error**" and "**relative**" for the x, y, ρ, and φ axes separately. Specifically, the DoG function for φ was defined in Equation 1. For variables on the x, y, and ρ axes, a linear fitting function relates x ("**relative**") to y ("**error**"), by:

$$y = ax + b \quad (2)$$

As the orientation serial dependence effect analysis, we normalized the response error within each participant and combined all participants' data.

Central tendency effect in location perception

The central tendency effect only exists in noncircular variables, which are variables on the x, y, and ρ axes. For each participant, the same trials in the serial dependence effect analysis were chosen so that the two effects were comparable in later analysis. We characterized the relationship between response error and current stimulus location to quantify the central tendency effect. Previous studies on magnitude estimation discovered the linear relationship between response error and current stimulus (Petzschner et al., 2015), but we found that the raw data pattern was more complicated than the linear relationship, suggesting an alternative model. Therefore, we proposed a model called the "complex central tendency model (complex CT)" to capture the relationship between the current stimulus location (x) and the response error (y) with parameters a to e:

$$y = ax + b\sin(cx + d) + e \quad (3)$$

The classic linear model (linear CT) relating the current stimulus location (x) to response error (y) with parameters a and b was given by:

$$y = ax + b \quad (4)$$

As the serial dependence effect analysis, we normalized the response error within participants

and combined all participants. We used the corrected Akaike information criterion (AICc) to compare model performance (see Statistical analysis) and we found that the complex central tendency model outperformed the linear central tendency model for all three axes (see Results). Therefore, we used the complex CT model to fit the central tendency data in the following analysis.

Modeling serial dependence and central tendency

To test whether the long-term central tendency effect and the short-term serial dependence effect coexisted in the same trial, we proposed the compound model, including both the serial dependence and central tendency effect, given by:

$$y = ax_1 + b + cx_2 + dsin\,(ex_2 + f) \quad (5)$$

In Equation 5, y is the response error, x_1 is relative, x_2 is the current stimulus location, and a to f are free parameters. If the compound model outperformed both the complex CT model and the serial dependence model (SD), it would support the coexistence of two effects in one trial. Because the central tendency effect only exists for noncircular variables such as the x, y, and ρ axes, we proposed the compound model as a combination of linear serial dependence effect and complex central tendency effect for the x, y, and ρ axes.

Coordinates comparison

We compared two coordinate systems' goodness of fit in explaining the serial dependence and central tendency effects. In all, we have five candidate models to describe the serial bias: the SD, linear central tendency model (linear CT), complex central tendency model (complex CT), compound model (complex CT + SD), and a constant model with a constant bias (constant). We added the AICc of the best models among five candidates for the x and y axes to get the AICc of Cartesian coordinates. We added the AICc of the best model among five candidates for the ρ axis and the best model among two candidates for φ axis (constant/DoG serial dependence) to get the AICc of the polar coordinates. We then compared the AICc of the two coordinates.

Statistical analyses

For these models, the linear model fitting was conducted using the *fitlm* function ("statistics and machine learning" toolbox), which uses an iteratively reweighted least squares algorithm. The nonlinear model fitting was conducted with the *fitnlm* function, which uses the Levenberg–Marquardt nonlinear least squares algorithm. We used the Bayesian model comparison method, using the index AICc (Hurvich & Tsai, 1989) to select the best model among several candidate models, that is, the model with the lowest AICc. We subtracted the best model's AICc from each model's AICc to get the $\Delta AICc$. If the difference in AICc between two models is greater than 10, it suggests strong evidence in favor of the model with lower AICc (Burnham & Anderson, 2004).

For the serial dependence analysis, we also used the permutation test that was typically applied to assess whether there was a significant effect in previous studies. First, we shuffled the trial sequence of raw data and fitted the SD to the permuted data. The shuffle and fitting process was conducted 5,000 times. The adjusted R^2 of those fittings formed a null distribution against which the adjusted R^2 of raw data's fitting were compared. The P value was taken as the proportion of adjusted R^2 in null distribution, which was larger than or equal to the raw data's fitting adjusted R^2.

Furthermore, because the statistical analysis was conducted on the aggregated data, to account for the random effect caused by variance across participants, we also conducted a mixed effect analysis with the *fitglme* function and *nlmefit* function on the offline experiment data (experiments 1 and 4).

Results

Four experiments were performed to examine the spatial coordinates for serial bias in 2D continuous space. As illustrated in Figure 1A, subjects were presented with a target stimulus (Gabor patch in experiment 1, black dot in experiments 2–4) followed by a mask (square mask in experiments 1, 3, and 4; round mask in experiment 4) in each trial, and were instructed to perform a position adjustment task by using keyboards (experiments 1–3) or a mouse (experiment 4).

Replication of the orientation SD effect (experiment 1)

In experiment 1, different from experiments 2 to 4, participants needed to reproduce both the location and orientation of a Gabor patch (Figure 1A). The additional orientation task was to validate the data quality and analysis methods in the present study. As shown in Figure 1B, experiment 1 replicated the typical orientation serial dependence effect (e.g., Cicchini, Mikellidou, & Burr, 2018; Fischer et al., 2020; Fischer & Whitney, 2014; Fritsche et al., 2017). Specifically, the reported orientation in the current trial was biased toward the previously presented orientation, i.e., an

attractive effect that follows a DoG shape pattern ($\Delta AICc = 252.4$, model comparison against constant model; adjusted $R^2 = 0.0112$, $P = 10^{-4}$, permutation test).

Characterizing serial bias in spatial perception in two coordinates (experiment 1)

After confirming the serial dependence for orientation features, we next examined the effect on 2D continuous spatial location by examining how the perceived location in the current trial is influenced by the position of the previous grating. Importantly, we quantified the cross-trial spatial bias effect in both Cartesian (red box; Figure 1C) and polar coordinates (blue box; Figure 1F). Specifically, the dependence of the response error in the current trial on the previously presented position as well as on the overall central trend, referred to as serial dependence and central tendency effect respectively, could be characterized by x and y in the Cartesian coordinates (Figure 1C) and by ρ and φ in the polar coordinates (Figure 1F). We next built five candidate models to characterize the spatial serial bias (Figure 1I): a constant model with constant biases (Constant), a SD, a linear central tendency model (linear CT), a complex central tendency model (complex CT), and a compound model comprising serial dependence and complex central tendency effects (SD + complex CT).

First, the serial dependence effect on location exhibited an attractive bias in both coordinates (Figure 1DG). In the Cartesian coordinates, the perceived target location in the current trial was pulled in the direction of the grating position in the preceding trial, at both the x and y axis. Specifically, as shown in Figure 1D, the perception error was positively proportional to the target location shift across consecutive trials (SD model vs. Constant model; x: $\Delta AICc = 2418.8$; y: $\Delta AICc = 3824.7$). Similarly, in the polar coordinates (Figure 1G), the perception error defined at ρ axis also showed a positive linear pattern (SD model vs. constant model; $\Delta AICc = 1382.8$). The serial dependence effect for φ followed a DoG-shaped curve($\Delta AICc = 266.6$), consistent with previous findings (Bliss et al., 2017; Manassi et al., 2018). Permutation tests further supported significant serial dependence for all the parameters in the two coordinates ($P = 10^{-4}$ for all axes).

The central tendency effect occurred as well, for both coordinates (Figure 1EH). Specifically, the x axis and y axis in the Cartesian coordinates and the ρ axis in the polar coordinates revealed a linear relationship between the position error and the shift of target location from the center. Note that the φ axis in the polar coordinates was not applicable to quantify the central tendency effect (right panel, Figure 1H). Given that the complex CT model surpassed both the linear CT model (X: $\Delta AICc = 1118.5$; Y: $\Delta AICc = 224.8$; ρ: $\Delta AICc = 128.2$) and the constant model (X: $\Delta AICc = 4104.3$; Y: $\Delta AICc = 5290.3$; ρ: $\Delta AICc = 1541.3$), we used the complex CT model in the subsequent analyses.

To test whether the two effects—serial dependence and central tendency effect—concurrently occurred in the same trial, we built a compound model (SD + complex CT). The model comparison between the compound model and the single effect models (SD or complex CT) indeed supported the coexistence of two effects for x, y, and ρ (Figure 1I) (compound model vs. SD model: $\Delta AICc = 1951.7$ for X; $\Delta AICc = 1807.8$ for Y; $\Delta AICc = 394.5$ for ρ; compound model vs. complex CT model: $\Delta AICc = 266.2$ for X, $\Delta AICc = 342.2$ for Y; $\Delta AICc = 236.0$ for ρ).

Cartesian outperforms polar coordinates in characterizing spatial serial bias (experiment 1)

Figure 1I summarizes the model comparison results, for the four parameters (Cartesian coordinates: x and y; polar coordinates: ρ and φ) and the five different models (Constant, SD, linear CT, complex CT, SD + complex CT). Importantly, for all the three noncircular variables (x, y, ρ), the SD + complex CT model outperformed the other four models (denoted by ※), suggesting that spatial perception involves concurrent serial dependence and central tendency effect. Note that because the circular variable φ was not applicable for the central tendency effect, it only applied to the constant and SD models and was denoted in the other three models by ⊘.

Finally, we compared the two coordinates in their abilities to quantify the serial bias in 2D continuous spatial perception. We chose the goodness of fit value (AICc) of the best model for each of the four parameters (x, y, ρ, and φ) and added the values belonging to the same coordinates respectively (Cartesian coordinates: x and y; polar coordinates: ρ and φ). As shown in Figure 1J, the Cartesian coordinates performed better than the polar coordinates ($\Delta AICc = 7959.2$). Furthermore, a mixed effect analysis that considers random effect also supports that Cartesian outperforms Polar coordinates (Supplementary Figure S1A). Therefore, stable spatial perception in a 2D continuous space over time is better characterized via Cartesian rather than Polar coordinates.

Cartesian coordinate engages in spatial serial bias rapidly (experiment 2)

In experiment 1, we found that the Cartesian coordinates engage the serial bias in 2D continuous spatial perception. In experiment 2, we tested whether the finding is a general phenomenon and could persist in

		Constant	SD	Linear CT	Complex CT	SD + Complex CT
Experiment 2						
Cartesian	x	1940.618	1561.0	1359.4	14.9	0
	y	1247.2	621.5	431.8	50.4	0
Polar	ρ	1078.1	413.0	154.9	40.0	0
	φ	36.6	0			
Experiment 3						
Cartesian	x	1703.9	1239.0	1183.6	46.9	0
	y	1363.9	636.6	355.5	42.8	0
Polar	ρ	786.3	246.1	99.3	45.9	0
	φ	43.7	0			
Experiment 4						
Cartesian	x	6070.0	3230.2	1525.7	95.6	0
	y	8556.2	3934.0	568.5	116.9	0
Polar	ρ	3077.6	1603.1	56.9	0	1.8
	φ	49.5	0			

Table 1. Model comparison results of experiments 2–4 (ΔAICc compared with the best model on each axis).

more natural environments, that is, online experiments. Moreover, because the online experiments are limited in the number of trials that could be tested per subject, we also examined whether the engagement of Cartesian coordinates emerges in a short time.

To this end, we conducted a comparable online and short experiment (50 trials per subject) as experiment 1 (Figure 2A). Because the orientation serial dependence has been replicated in experiment 1, we chose to focus on the spatial bias by only asking subjects to perform a spatial position adjustment task using keyboards. The same analysis was performed. As shown in the middle and right panels of Figure 2A, similar results as experiment 1 were found. Specifically, the serial dependence and central tendency effects occurred (the see detailed model comparison results in Table 1), and, most important, consistent with experiment 1, the Cartesian coordinates outperformed the polar coordinates ($\Delta AICc = 2073.1$). Therefore, the role of the Cartesian coordinates in mediating serial bias in continuous 2D spatial perception does not rely on strictly controlled environmental settings as well as lengthy tests, but instead emerges rapidly in a natural context.

Engagement of Cartesian coordinates is not due to spatial contexts (experiment 3)

A possible confounding factor for the role of the Cartesian coordinate observed in experiments 1 and 2 is the shape of the mask that follows the target stimulus. The square mask might establish certain spatial contexts in which subjects tend to use the Cartesian coordinates for spatial perception. To address this question, we performed experiment 3, the design of which was exactly the same as experiment 2 (online experiment, 50 trials per subject) except that a round-shaped mask was presented after the target (left panel, Figure 2B). Given that a round shape would be more naturally linked to polar rather than Cartesian coordinates, we could examine whether the serial bias in spatial perception would be better characterized via the polar coordinates in this new experimental setting.

As shown in the middle and right panels of experiment 2B, similar results were found (see the detailed model comparison results in Table 1). Most crucially, the Cartesian still outperformed the polar coordinate ($\Delta AICc = 2237.8$), suggesting that the role of the Cartesian coordinates in serial bias in continuous 2D spatial perception is not due to the spatial context the following mask might bring about. Instead, the function of the Cartesian coordinates persists even in spatial contexts that likely favor the polar coordinate.

Engagement of Cartesian coordinates is not due to response modality (experiment 4)

For experiments 1, 2, and 3, subjects were instructed to use four keys (‘w,’ ‘s,’ ‘a,’ and ’d’) on the keyboard, both offline and online, to adjust the probe position to match that of the target. Therefore, the response keys might potentially form a quadrangular grid-like form (i.e., left, right, up, down), which would facilitate the role of Cartesian coordinates in 2D spatial perception. To address this confounding factor, in experiment 4, subjects were instructed to use the mouse to perform the spatial reproduction task, that is, moving the mouse to the target location (left panel, Figure 2C). Because the mouse response follows a naturally continuous trajectory in a 2D space and would not be constrained

by the quadrangular grid-like pattern when using keyboards, we would expect disrupted Cartesian coordinates' role if the keyboard-based response modality had shaped the spatial coordinates in previous experiments.

As shown in Figure 3C (middle and right panels), experiment 4 displayed similar results as before. Again, subjects' serial position perception showed both serial dependence and central tendency effects, which coexisted in the same trial (see the details for model comparisons results in Table 1). Most important, the Cartesian coordinates still outperformed the polar coordinates in characterizing the serial bias effect ($\Delta AICc = 11499.5$). A mixed-effect analysis that considers random effect supports the same conclusion (Supplementary Figure S1B). Therefore, the engagement of Cartesian coordinate in stable spatial perception over time is not due to the response modality either.

Discussion

The goal of the present study was to examine the spatial coordinates of serial bias in continuous 2D spatial perception. To this end, we performed four experiments with varying factors, that is, experiment context (online vs. offline), test length (long vs. short), spatial context (shape of the visual mask), and response context (keyboard vs. mouse), which convergingly demonstrate that serial biases in spatial perception—serial dependence and central tendency effect—are better characterized by Cartesian than polar coordinates. Taken together, Cartesian coordinates scaffold the spatiotemporal integration process in continuous 2D spaces to help perceptual stability, supporting the involvement of allocentric reference frame and top–down modulation in spatial perception over long time intervals.

Our results revealed a positive serial dependence effect in location perception, such that the target position seems to be pulled toward the previously encountered location. This attractive effect has been found for a wide range of features, including orientation (Cicchini et al., 2018; Fischer & Whitney, 2014; Fritsche et al., 2017, Fritsche et al., 2020), numerosity (Cicchini, Anobile, & Burr, 2014), and motion (Alais, Leung, & Van der Burg, 2017). Prior work has also shown an attractive effect on spatial position over trials (Bliss et al., 2017; Manassi et al., 2018), but by testing targets on an isoeccentric circle. Here we replicated and extended the findings to continuous 2D spaces that are more commensurate with daily visual experiences, thus supporting a general function of attractive serial dependence in spatial perception. In addition to serial dependence, we revealed another relatively long-term serial bias effect, that is, the central tendency effect, which has been observed in magnitude perception (Allred et al., 2016; Petzschner et al., 2015; Sciutti et al., 2012). Therefore, past spatial experience lingers and integrates with current inputs, as manifested in serial dependence and central tendency effect, to help advance the perceptual stability in visual experiences (Cicchini et al., 2018; Petzschner et al., 2015).

The serial dependence effect has been viewed as an adaptive smoothing process by forming a continuity field over space and time (Fischer & Whitney, 2014; Liberman et al., 2014), yet the spatial coordinates underlying this spatiotemporal continuity kernel remain unknown. Here four experiments consistently revealed that the Cartesian coordinate outperforms the Polar coordinate in characterizing serial dependence and central tendency effects in continuous 2D spatial perception, regardless of experimental context (online vs. offline), spatial context (shape of the mask; square vs. round), and response context (keyboard vs. mouse). Moreover, the superiority of Cartesian coordinates does not rely on extensive experiences and could emerge rapidly, that is, within only 50 trials, further supporting its fundamental role in spatiotemporal integration. Interestingly, a recent study shows that serial dependence in color builds up through the experimental session (Barbosa & Compte, 2020), that is, weak or even no serial dependence at the beginning of the experiment. The rapid emergence of serial dependence in spatial perception thus supports the fundamental and automatic spatiotemporal continuity.

The quantitative comparison between Cartesian and polar coordinates could help to elucidate the operation stage of serial dependence in spatial perception, which by itself has been found to entail either Cartesian or polar coordinates in varying contexts. Attneave and Curlee (1977) revealed Cartesian-based organization in a multidot spatial pattern reproduction task, whereas Zetzsche and colleagues (1999), in a Gabor patch discrimination task, showed evidence favoring polar coordinates. They proposed that the polar coordinate would be beneficial in the early stages of visual processing, given its efficiency in removing the statistical redundancies of natural images (Zetzsche et al., 1999). Yang (2018) revealed that Cartesian and polar representations could be used flexibly under different task conditions. Specifically, the Cartesian coordinate dominates when saccades are used to reproduce spatial location, whereas the polar coordinate is better when subjects are asked to point to the target position while maintaining central fixations. Overall, polar and Cartesian coordinates might be associated with early and late visual processing stages, respectively, with the former being retinotopic and eye centered to maximize discrimination of visual features, whereas the latter are optimal for stabilizing visual experiences when eyes move. This finding is consistent with the serial

dependence literature that repulsive adaptation-like serial bias reflects efficient information processing at the low-level stage, whereas attractive serial dependence operates at a postperceptual level to stabilize the interpretation of the outside world (Fritsche et al., 2017; Fritsche et al., 2020; Pascucci et al., 2019).

To our knowledge, no previous studies have examined the spatial coordinates for serial bias in 2D continuous spatial perception. Nevertheless, our findings are in line with the prior work showing that serial dependence on orientation acts in an allocentric (world-centered or spatiotopic) way (Mikellidou et al., 2021). Serial dependence is viewed as an optimal integration process that could be described by an ideal Bayesian observer model (Fritsche et al., 2020), and because the visual environment tends to be stable over time, this integration process would efficiently alleviate our cognitive loads (Cicchini et al., 2018). In principle, the temporal smoothing process needs to be world centered to resist retinal image changes and advance continuous visual experiences. It is found that the consciously perceived information (Kim et al., 2020; Pascucci et al., 2019; Zhang & Alais, 2020), working memory, and feedback from higher areas (Cicchini, Benedetto, & Burr, 2021; Fritsche et al., 2017) would influence subsequent perception, advocating the involvement of higher processing stages that are presumably more spatiotopic in serial bias (Burr & Morrone, 2011; McKyton & Zohary, 2007). Thus, the Cartesian coordinate serves as a reliable spatiotopic, world-centered system to facilitate temporal redundancy reduction when prior spatial experience integrates with current information in continuous 2D spaces.

Finally, in addition to serial bias that occurs at relatively long temporal scales (e.g., cross trials), there are also trans-saccadic spatial updating mechanisms to achieve stability in a spatiotopic (world-centered) manner (Burr & Morrone, 2011; Drissi-Daoudi et al., 2020; Fabius et al., 2019; Fairhall et al., 2017). This trans-saccadic spatial smoothing process presumably occurs in the Cartesian coordinates as well. The Cartesian and polar coordinates mainly differ in their primitive units, that is, rectangular grids of equal size for Cartesian and unequaled grids for polar (Yang, 2018). The even distribution characteristics endow the Cartesian coordinate with the capability to form optimal global representations instead of being biased to reference points as the polar coordinate does. Thus, by integrating polar-based representation at early stages to deal with detailed information around the fovea and Cartesian-based spatiotopic representations at late stages, our perceptual system is capable of processing local details while at the same time maintaining stable global representations. Different from the fast operation of saccades (3 times per second), serial dependence takes place up to tens of seconds, during which many saccades could be made. Overall, the similar temporal smoothing principle and the spatial coordinate system might underlie perception stability over both short and long time intervals.

Taken together, the present study, in four experiments, provides converging new evidence supporting that the serial bias in spatial perception operates in Cartesian coordinates. Past spatial experiences are represented, maintained, and integrated into current information over time, which is organized in a Cartesian coordinate, to achieve steady representations of the external world.

Keywords: spatial perception, serial dependence, central tendency, Cartesian coordinates, polar coordinates

Acknowledgments

Supported by the National Science and Technology Innovation 2030 Major Program 2021ZD0204103 to H.L., National Natural Science Foundation of China (31930052) to H.L., China Postdoctoral Science Foundation (2020M680166 to H.Z.), and Peking University Boya Postdoctoral Fellowship (to H.Z.).

Author contributions: M.L., H.Z., and H.L. designed the experiment. M.L. performed behavioral experiments and data analysis, and prepared figures. M.L., H.Z., and H.L. wrote the paper.

Commercial relationships: none.
Corresponding authors: Huihui Zhang; Huan Luo.
Emails: huihuizhang@pku.edu.cn; huan.luo@pku.edu.cn.
Address: School of Psychological and Cognitive Sciences, Peking University, PKU-IDG/McGovern Institute for Brain Science, Peking University, Room 1703, 52 Haidian Road, Beijing, 100087, China.

References

Alais, D., Leung, J., & Van der Burg, E. (2017). Linear summation of repulsive and attractive serial dependencies: Orientation and motion dependencies sum in motion perception. *Journal of Neuroscience, 37*(16), 4381–4390.

Allred, S. R., Crawford, L. E., Duffy, S., & Smith, J. (2016). Working memory and spatial judgments: Cognitive load increases the central tendency bias. *Psychonomic Bulletin & Review, 23*(6), 1825–1831.

Attneave, F., & Curlee, T. E. (1977). Cartesian organization in the immediate reproduction of spatial patterns. *Bulletin of the Psychonomic Society, 10*(6), 469–470.

Barbosa, J., & Compte, A. (2020). Build-up of serial dependence in color working memory. *Scientific Reports, 10*(1), 1–7

Bliss, D. P., Sun, J. J., & D'Esposito, M. (2017). Serial dependence is absent at the time of perception but increases in visual working memory. *Scientific Reports, 7*(1), 14739.

Brainard, D. H. (1997) The Psychophysics Toolbox, *Spatial Vision, 10*, 433–436.

Burr, D., & Cicchini, G. M. (2014). Vision: Efficient adaptive coding. *Current Biology, 24*(22), R1096–R1098.

Burr, D. C., & Morrone, M. C. (2011). Spatiotopic coding and remapping in humans. *Philosophical Transactions of the Royal Society B: Biological Sciences, 366*(1564), 504–515.

Burnham, K. P., & Anderson, D. R. (2004). Multimodel inference: Understanding AIC and BIC in model selection. *Sociological Methods & Research, 33*(2), 261–304.

Cicchini, G. M., Anobile, G., & Burr, D. C. (2014). Compressive mapping of number to space reflects dynamic encoding mechanisms, not static logarithmic transform. *Proceedings of the National Academy of Sciences of the United States of America, 111*(21), 7867–7872.

Cicchini, G. M., Benedetto, A., & Burr, D. C. (2021). Perceptual history propagates down to early levels of sensory analysis. *Current Biology, 31*(6), 1245–1250.

Cicchini, G. M., Mikellidou, K., & Burr, D. C. (2018). The functional role of serial dependence. *Proceedings of the Royal Society B, 285*(1890), 20181722.

Collins, T. (2019). The perceptual continuity field is retinotopic. *Scientific Reports, 9*(1), 1–6.

Drissi-Daoudi, L., Öğmen, H., Herzog, M. H., & Cicchini, G. M. (2020). Object identity determines trans-saccadic integration. *Journal of Vision, 20*(7), 33–33.

Fabius, J. H., Fracasso, A., Nijboer, T. C., & Van der Stigchel, S. (2019). Time course of spatiotopic updating across saccades. *Proceedings of the National Academy of Sciences of the United States of America, 116*(6), 2027–2032.

Fairhall, S. L., Schwarzbach, J., Lingnau, A., Van Koningsbruggen, M. G., & Melcher, D. (2017). Spatiotopic updating across saccades revealed by spatially-specific fMRI adaptation. *Neuroimage, 147*, 339–345.

Fischer, C., Czoschke, S., Peters, B., Rahm, B., Kaiser, J., & Bledowski, C. (2020). Context information supports serial dependence of multiple visual objects across memory episodes. *Nature Communications, 11*(1), 1–11.

Fischer, J., & Whitney, D. (2014). Serial dependence in visual perception. *Nature Neuroscience, 17*(5), 738–743.

Fritsche, M., Mostert, P., & de Lange, F. P. (2017). Opposite effects of recent history on perception and decision. *Current Biology, 27*(4), 590–595.

Fritsche, M., Spaak, E., & De Lange, F. P. (2020). A Bayesian and efficient observer model explains concurrent attractive and repulsive history biases in visual perception. *Elife, 9*, e55389.

Gallistel, C. R. (1990). *The organization of learning*. Cambridge, MA: The MIT Press.

Hurvich, C. M., & Tsai, C. L. (1989). Regression and time series model selection in small samples. *Biometrika, 76*(2), 297–307.

Kim, S., Burr, D., Cicchini, G. M., & Alais, D. (2020). Serial dependence in perception requires conscious awareness. *Current Biology, 30*(6), R257–R258.

Klatzky, R. L. (1998). Allocentric and egocentric spatial representations: Definitions, distinctions, and interconnections. In: *Spatial cognition* (pp. 1–17). Berlin, Heidelberg: Springer.

Li, Q., Joo, S. J., Yeatman, J. D., & Reinecke, K. (2020). Controlling for participants' viewing distance in large-scale, psychophysical online experiments using a virtual chinrest. *Scientific Reports, 10*(1), 904, doi:10.1038/s41598-019-57204-1.

Liberman, A., Fischer, J., & Whitney, D. (2014). Serial dependence in the perception of faces. *Current Biology, 24*(21), 2569–2574.

Manassi, M., Liberman, A., Kosovicheva, A., Zhang, K., & Whitney, D. (2018). Serial dependence in position occurs at the time of perception. *Psychonomic Bulletin & Review, 25*(6), 2245–2253.

Manassi, M., & Whitney, D. (2022). Illusion of visual stability through active perceptual serial dependence. *Science Advances, 8*(2), eabk2480.

McKyton, A., & Zohary, E. (2007). Beyond retinotopic mapping: the spatial representation of objects in the human lateral occipital complex. *Cerebral Cortex, 17*(5), 1164–1172.

Mikellidou, K., Cicchini, G. M., & Burr, D. C. (2021). Perceptual history acts in world-centred coordinates. *i-Perception, 12*(5), 1–7.

Motala, A., Zhang, H., & Alais, D. (2020). Auditory rate perception displays a positive serial dependence. *i-Perception, 11*(6), 2041669520982311, https://doi.org/10.1177/2041669520982311.

Pascucci, D., Mancuso, G., Santandrea, E., Libera, C. D., Plomp, G., & Chelazzi, L. (2019). Laws of concatenated perception: Vision goes for novelty, decisions for perseverance. *PLoS Biology, 17*(3), e3000144.

Peirce, J. W., Gray, J. R., Simpson, S., MacAskill, M. R., Höchenberger, R., & Sogo, H., . . .Lindeløv, J. (2019). PsychoPy2: Experiments in behavior made easy. *Behavior Research Methods, 51*(1), 195–203, doi:10.3758/s13428-018-01193-y.

Pelli, D. G. (1997) The VideoToolbox software for visual psychophysics: Transforming numbers into movies, *Spatial Vision, 10*, 437–442.

Petzschner, F. H., Glasauer, S., & Stephan, K. E. (2015). A Bayesian perspective on magnitude estimation. *Trends in Cognitive Sciences, 19*(5), 285–293.

Rucci, M., Ahissar, E., & Burr, D. (2018). Temporal coding of visual space. *Trends in Cognitive Sciences, 22*(10), 883–895.

Sciutti, A., Del Prete, A., Natale, L., Sandini, G., Gori, M., & Burr, D. (2012) Central tendency in space perception varies in development and is altered in human-robot interactive tasks. Paper presented at Humanoids 2012 Workshop on Developmental Robotics, Osaka, Japan.

Sheth, B. R., & Shimojo, S. (2001). Compression of space in visual memory. *Vision Research, 41*(3), 329–341.

Whitney, D. (2002). The influence of visual motion on perceived position. *Trends in Cognitive Sciences, 6*(5), 211–216.

Yang, F. (2018). The formats of position representations in vision (Doctoral dissertation). Baltimore, MD: Johns Hopkins University.

Zetzsche, C., Krieger, G., & Wegmann, B. (1999). The atoms of vision: Cartesian or polar? *JOSA A, 16*(7), 1554–1565.

Zhang, H., & Alais, D. (2020). Individual difference in serial dependence results from opposite influences of perceptual choices and motor responses. *Journal of Vision, 20*(8), 2–2.